An SPH-based elastic-column model for transients in rapid emptying of pipelines

Qingzhi Hou[1,2], Arris S. Tijsseling[3], Soon-Thiam Khu[4]
[1] School of Civil and Transportation Engineering, Qinghai Minzu University, Xining 810007, China
[2] State Key Laboratory of Hydraulic Engineering Simulation and Safety, Tianjin University, Tianjin 300350, China
[3] Department of Mathematics and Coumputer Science, Eindhoven University of Technology, Eindhoven 5600 MB, The Netherlands
[4] School of Environmental Science and Engineering, Tianjin University, Tianjin 300350, China

ABSTRACT

This paper reports the development and application of an elastic-column model for rapid draining of pipelines. The water-hammer equations with a moving boundary are used to model the emptying process, and the SPH method is employed to solve the governing equations. The image particle method is used to ensure complete kernel support and impose boundary conditions, simultaneously. The velocity-Verlet method is applied for time integration to enhance accuracy. The developed SPH-based elastic-column model clearly shows the transient effect in the emptying process, and it is a promising tool for the simulation of rapid emptying of pipelines with undulating elevation profiles.

1 INTRODUCTION

Fast transient flow in piping systems is generally caused by rapid changes in flow conditions due to sudden valve operation, pump start up or shut down, and power failure. This phenomenon is known as pressure surge or water hammer, and it may damage hydraulic machinery, piping and supports. If possible, it should be anticipated in the design process and prevented in practice (1). Fast transients may also occur in rapid pipe filling and emptying processes, for which a recent literature review is presented by Fuertes-Miquel et al. (2). Rapid pipe filling and emptying occur in various hydraulic applications, such as water-distribution networks, storm-water and sewage systems, fire-fighting systems, oil transport pipelines and pipeline cleaning. With respect to rapid filling of an empty pipeline, while the water column is driven by a high head, air is expelled by the advancing water column. If the air flow is not blocked, the water column grows with little adverse pressure and attains a high velocity. For emptying of a pipeline initially filled with water, while the air is blown into the pipeline, water is expelled out of the system. If the driving air pressure is high and the resistance from pipe components is low, the water

column shortens and attains a high velocity. When the advancing column is suddenly stopped (fully or partially), severe pressure changes occur in the system. A reliable model that can predict the change of the water column velocities and the induced overpressure in the system is desirable.

The pipe *filling* processes have been mostly focused on and the models have shown great accuracy in comparison to experimental data. For the modelling of the rapid filling of pipelines, the rigid-column theory is commonly used. The rigid-column filling model for pipes in series was formulated in (3). The model describes the unsteady motion of a lengthening water column filling empty pipelines with an undulating elevation profile. The model was validated against laboratory tests and extended to represent a branched system with undulating pipe segments (5). By coupling the rigid-column model with an entrapped air model, Cabrera et al. (6) addressed filling pipes with initial air entrapped between water columns. The rigid-column model gave good results as long as the flow remains axially uniform. When the water column is disturbed somewhere in the system, pressure oscillations along its length or even column separation may occur and the rigid-column model will fail. The elastic model for unsteady flow in conduits is capable of dealing with potential fast transients in rapid pipe filling. However, the elastic model with a moving boundary is difficult to solve using traditional mesh-based methods. A recent attempt is the fully implicit box or Preissmann finite-difference scheme of Malekpour and Karney (7). This method uses a fixed spatial grid and a flexible temporal grid, and hence the Courant number is time dependent. The obtained results gave acceptable agreement with the laboratory tests of Liou and Hunt (3). However, a serious and unsolved numerical convergence problem occurred due to an uncontrollable large Courant number. To solve this problem, the method of characteristics (MOC) was applied by Malekpour and Karney (8). Since both the spatial and temporal grid are fixed in the MOC, the Courant number is constant and an interpolation has to be used to deal with the increasing water-column length. To better track the moving water-air interface and capture the transient effect without interpolation in MOC (8), Liu et al. (9) proposed a rigid-plug elastic water model, in which the water segment within two grid points is treated as a rigid column and the rest of the water column is simulated by the elastic model. To treat the transients in the whole water column, Hou et al. (10) developed an SPH-based elastic model, validated it against the experiments of Liou and Hunt (3) and then extended it for rapid filling of a pipe with entrapped air pocket (11). Taking the mass shedding at the water-air interface into account, Tijsseling et al. (12) proposed an improved rigid-column model for rapid filling and validated it against experiments in a large-scale pipeline (13,14,15,16), and further applied it to rapid filling with venting entrapped gas (17).

The pipe *emptying* problem has not received much attention in the literature because it often occurs together with other hydraulic phenomena (2,12,15,18). Different from pipe filling, the air is under pressure and the interaction between air and water plays an important role in the draining process. In the case of pipeline emptying with compressed air supplied from the upstream end as studied by Laanearu et al. (15,16), the moving water column is pressurized and its tail becomes stratified flow, i.e., mixed flow situations are possible. Pipe emptying experiments for a small-scale single pipe (19) and a large-scale undulating pipe (16) were performed to study two-phase flow transitions. Coronado-Hernandez et al. (20) developed a rigid-column model for rapid emptying and validated it against the large-scale experiments (13,14,15,16). To obtain results comparable with the measurements, the length of the pipe and the friction factor were adjusted irrationally (21). Recently, using the rigid-column model developed in (20), Coronado-Hernandez et al. (22) studied the sub-atmospheric pressure in a water-draining pipeline with an air pocket.

To accurately capture the transient phenomenon in rapid emptying of pipelines and to better understand its mechanism and examine the influencing factors, an elastic-column

model has to be used. In this model, the transients are governed by the waterhammer equations with moving boundary, for which numerical difficulties are inevitable for mesh-based Eulerian methods. However, it can be conveniently solved by the smoothed particle hydrodynamics (SPH) (10,11), which is a meshless Lagrangian method. In this work, a SPH-based elastic-column model is developed for the rapid emptying of pipelines with undulating elevation profiles.

2 SPH-BASED ELASTIC-COLUMN MODEL

2.1 Problem statement and governing equations

For the emptying of a pipeline with undulating elevation profile, consider a pipeline with two valves and an upstream air tank as sketched in Fig. 1. Water is initially filled in the pipe between the upstream tank (filled with pressurized air) and the closed downstream valve. When the downstream valve is opened, the water is expelled out of the system due to the pressurized air. This is an illustration of the pipe draining experiments (14,19).

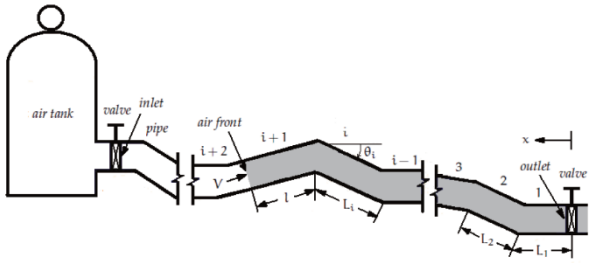

Figure 1 – Sketch of the draining of a pipeline with undulating elevation profile

The flow is treated as one-dimensional, and hence the governing continuity equation in Lagrangian form is

$$\frac{d\rho}{dt} = -\rho \frac{\partial u}{\partial x} \tag{1}$$

where d/dt is the total derivative, u is the cross-sectional averaged velocity, ρ is the density, x and t are spatial and temporal coordinate, respectively.
From the equation of state

$$p - p_0 = c^2(\rho - \rho_0) \tag{2}$$

we can obtain

$$\frac{dp}{dt} = -c^2 \frac{d\rho}{dt} \tag{3}$$

where p is the pressure, c is the sound speed, and ρ_0 is the reference density at the reference pressure p_0.

Substituting Eq. (3) into Eq. (1) yields the continuity equation in term of pressure as

$$\frac{dp}{dt} = -\rho c^2 \frac{\partial u}{\partial x} \tag{4}$$

The liquid compressibility and pipe wall elasticity have been taken into account through the wave speed, while the density in Eq. (4) is taken constant. Assume that the filled pipes remain full and a well-defined water-air interface exists. Then the momentum equation with Darcy-Weisbach friction is

$$\frac{du}{dt} = -\frac{1}{\rho}\frac{\partial p}{\partial x} + g\sin\theta - f\frac{u|u|}{2D} \tag{5}$$

where g is the gravitational acceleration, f is the friction factor and D is the pipe diameter. Note that u^2 instead of $u|u|$ can be used here because return flow does not occur during the rapid emptying process. Equations (4) and (5) are the classical waterhammer equations with two more convection terms in the total derivatives.

With regard to the friction factor, the Darcy-Weisbach friction law developed for steady turbulent flow is used. Although the validity of the traditional assumption of using steady friction has been challenged, it should not be an issue for the inertia driven problems studied herein. Different from (10), where a constant friction factor f was used, the friction factor used herein depends on the Reynolds number Re, which changes with the flow velocity. Its instantaneous value is calculated from

$$f = \begin{cases} 64, & 0 \le Re < 1 \\ \frac{64}{Re}, & 1 \le Re \le 2500 \\ 0.25\left[\log\left(\frac{\varepsilon/D}{3.7} + \frac{5.74}{Re^{0.9}}\right)\right]^{-2}, & Re > 2500 \end{cases} \tag{6}$$

where ε/D is the relative roughness and $Re \coloneqq uD/\nu$ with ν the kinematic viscosity. For turbulent flow ($Re > 2500$), the above expression is known as the Swamee-Jain formula. The relative roughness can be directly measured, provided by the manufacturer, or found in handbooks. The kinematic viscosity $\nu = 10^{-6}$ m2/s is used here for water.

Assume that the reference pressure p_0 in Eq. (2) is the atmospheric pressure, the initial conditions are

$$u(x,0) = 0, \quad p(x,0) = \rho g H_a + x\sin\theta \tag{7}$$

where H_a is the pressure head of the air tank. Note that all inclination angles need to be included for a pipe with undulating elevation profile.

The upstream side of the downstream valve is taken as the origin of the axial coordinate system. Then the boundary condition at the outlet is

$$p(0,t) = K_v\frac{\rho u_v^2}{2} \tag{8}$$

where K_v is the head loss coefficient accounting for valve resistance and u_v is the flow velocity upstream of the valve. The moving water-air interface condition for the shortening water-column after valve opening is

$$p(L_0 - L(t), t) = p_{inter} \tag{9}$$

where P_{inter} is the pressure at the water-air interface, L_0 is the initial water-column length, and $L(t)$ is the column length at time t, which is calculated by

$$L(t) = L_0 - \int_0^t u_{inter} dt \tag{10}$$

where u_{inter} is the velocity of the moving water-air interface. Air flow dynamics is not modelled here, in the sense that the upstream driving air pressure p_{inter} is a given function of time, which may be a constant.

2.2 Smoothed particle hydrodynamics

Smoothed particle hydrodynamics (SPH) is a meshless, Lagrangian, particle method that uses an approximation technique to calculate field variables like velocity, pressure, position, etc. Unlike traditional mesh-based methods, the SPH method uses a set of particles without predefined connectivity to represent a continuum system and thus it is easy to handle problems with complex geometries and interfaces. It does not suffer from mesh distortion and refinement problems that limit the usage of mesh-based methods for hydrodynamic problems with free surfaces and moving boundaries. As a Lagrangian method, SPH naturally tracks material history information due to movement of the particles (10,11).

In SPH particle approximation, the derivative of a one-dimensional function f is

$$\frac{\partial f_a}{\partial x} = \frac{\partial f}{\partial x}(x_a) = \sum_b \frac{m_b}{\rho_b}(f_a - f_b)\frac{dW_{ab}}{dx_a} \tag{11}$$

in which the derivative of the kernel for the cubic-spline widely used in SPH is

$$\frac{dW_{ab}}{dx_a} = \frac{\text{sign}(x_a - x_b)}{h^2}\begin{cases} -2q + 1.5q^2, & 0 \le q < 1, \\ -0.5(2-q)^2, & 1 \le q < 2, \\ 0, & q > 2 \end{cases} \tag{12}$$

where the subscripts a and b are the indices of particles, m_b and ρ_b are the mass and density of particle b, $W(x - x_b, h)$ is the kernel function with h the smoothing length, and $q = x_{ab}/h$ with $x_{ab} = x_a - x_b$ the distance between the particles.

Replacing the spatial derivatives in Eqs. (4) and (5) with the approximation (11) yields the SPH formulation of the water-hammer equations as

$$\frac{dp_a}{dt} = -c^2 \sum_b m_b (u_a - u_b)\frac{dW_{ab}}{dx_a} \tag{13}$$

$$\frac{du_a}{dt} = -\frac{1}{\rho^2}\sum_b m_b (p_a - p_b + \Pi_{ab})\frac{dW_{ab}}{dx_a} + g\,sin\,\theta_a - \frac{\lambda u_a |u_a|}{2D} \tag{14}$$

The fact that the density is nearly constant has been used in the derivation of Eqs. (13) and (14). To alleviate possible oscillations at sharp wave fronts, an artificial viscosity term Π_{ab} (10,11) has been added to Eq. (14), which has the following form:

$$\Pi_{ab} = \frac{-ch}{\rho} min\left(\frac{(u_a - u_b)(x_a - x_b)}{r_{ab}^2 + 0.01h^2};\ 0\right) \tag{15}$$

2.3 Numerical boundary conditions

The SPH pressure boundary concept proposed in (10,11) is employed to impose the boundary conditions (8) and (9). The essential ingredient is to properly complete the truncated kernel supports using image particles.

The enforcement of the boundary condition (8) is sketched in Fig. 2a. Suppose that at time t fluid particle 'o' is the one closest to the downstream end and that its velocity is u_o. To complete the kernel support associated with particle 'o', a set of particles with spacing d_0 is placed outside the pipe end. Their velocity is taken as u_o and their pressure is

$$p_o = K_v \frac{\rho u_o^2}{2} \tag{16}$$

The moving air-water interface condition (9) is imposed in a similar way. The illustration is shown in Fig. 2b. Suppose that at time t fluid particle 'f' represents the moving air-water interface and its velocity is u_f. To complete the kernel associated with particle 'f', a set of particles with spacing d_0 is placed upstream of the particle 'f'. Their velocity is u_f and their pressure is

$$p_f = p_{inter} \tag{17}$$

All the introduced image particles are referred to as pressure particles as they are used to impose pressure conditions. The number of pressure particles for each boundary, N_{pp}, depends on the radius of the kernel support, which is $2h$ for the cubic-spline. To meet the requirement that the kernel associated with any a fluid particle needs to be fully supported, an integer $N_{pp} = \lfloor 2h/d_0 \rfloor$ must be taken. Practically, $N_{pp} = 2$ is used, which satisfies the above requirement for all one-dimensional cases. When a fluid particle leaves the pipeline, it becomes an outlet particle and at the same time the most downstream particle is deleted.

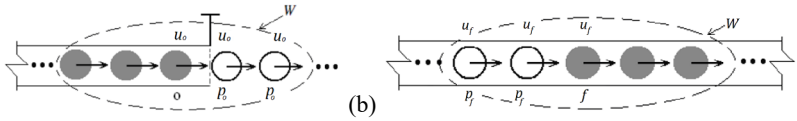

Figure 2 – Illustration of pressure particles for (a) downstream outlet and (b) moving water-air interface

2.4 Time integration and stability

The time derivatives in the SPH-based elastic model (13) and (14) are integrated by the velocity-Verlet method, which is second-order accurate and, more importantly, symplectic. The calculation process of the velocity-Verlet integral algorithm is given by

$$u_a^{n+1/2} = u_a^n + \frac{\Delta t}{2}\left(\frac{du_a}{dt}\right)^n \tag{18}$$

$$x_a^{n+1/2} = x_a^n + \frac{\Delta t}{2} u_a^{n+1/2} \tag{19}$$

$$p_a^{n+1} = p_a^n + \Delta t \frac{dp_a^{n+1/2}}{dt} \tag{20}$$

$$x_a^{n+1} = x_a^{n+1/2} + \frac{\Delta t}{2} u_a^{n+1/2} \tag{21}$$

$$u_i^{n+1} = u_i^{n+1/2} + \frac{\Delta t}{2}\left(\frac{du_i}{dt}\right)^{n+1} \tag{22}$$

where superscripts n, $n+1/2$ and $n+1$ represent the time levels.

For the velocity-Verlet scheme, the time step must satisfy the Courant-Friedrichs-Lewy (CFL) stability condition (23):

$$\Delta t \leq 0.25 \frac{h}{c+u_{max}} \tag{23}$$

where u_{max} is the maximum flow velocity in the simulation.

The time step size is not only crucial to stability, but also to accuracy and efficiency. If the time step is too large, instability occurs and accuracy reduces. On the other hand, unnecessary computation cost will be caused if the time step is too small. For optimization, a variable time step is taken here.

3 NUMERICAL RESULTS

To verify the SPH model for pipe emptying, we examine a physical setup as in the pipe filling experiment of Liou and Hunt (3). Differently, the water tank is replaced by an air tank, and the downstream end is equipped with a valve (see Fig. 1 with i = 1, 2). The two PVC pipes are initially full of water, which is at rest and under pressure. Two different cases are simulated. One is a small-scale case with short pipe and low driving head, and the other is a large-scale case with longer pipe and higher driving head.

3.1 Small-scale pipeline

In the first case, the air tank has a constant head of $H_a = 0.2$ m of water. The lengths of the two pipes are $L_1 = 3.55$ m and $L_2 = 3.11$ m, and their diameter is 22.9 mm. The inclination angles are $\theta_1 = 2.66°$ and $\theta_2 = 2.25°$ downward, respectively. The relative roughness is $\frac{\varepsilon}{D} = 0.00015$ and the sound speed c = 300 m/s. After the downstream valve opens instantaneously, water is driven out of the system by the constant air pressure and gravity. The resistance of the downstream valve is neglected, i.e., $K_v = 0$.

3.1.1 Velocity change

In SPH the selected particle spacing is $d_0 = \Delta x = 10$ mm, and hence there are initially 666 particles in the system. The simulation is terminated after the system is empty (after about 6 s). The predicted history of the averaged velocity and acceleration of the water particles is shown in Fig. 3 together with those obtained by the rigid-column model (19). The water column experiences rapid velocity changes at the early and late stages (Fig. 3a). The early rapid change is because of the low friction, and the late rapid change is because of the small column length (i.e., small mass). The velocity increases with shortening column length and experiences two rapid changes with large accelerations (Fig. 3b). At the early stage, inertia dominates and the water column accelerates at $(H_a + L_1 \sin + \theta_1 L_2 \sin\theta_2)/(L_1 + L_2) = 0.72$ m/s^2. When the velocity increases, friction becomes important and decreases the acceleration. When the column length is smaller, the friction force becomes less important again and the column experiences another rapid acceleration due to its small mass. This is clearly seen from the acceleration history shown in Fig. 3b. An inflection point exists in the velocity profile in Fig. 3a, which corresponds to the minimum acceleration exhibited in Fig. 3b. For both the averaged velocity and acceleration of the water column, the SPH simulation results agree well with the rigid-column solutions.

The computed velocity at the outlet is shown in Fig. 4a. Although fluctuations do exist in the early stage of the emptying process, the water elasticity effect is invisible without

zooming in. This is because the pipe length is too short. However, when one examines the maximum and minimum acceleration of the particles during pipe emptying, large variations due to liquid compressibility and pipe wall elasticity are clearly seen in Fig. 4b.

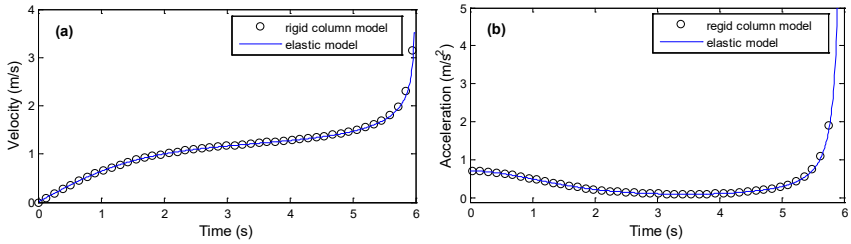

Figure 3 – History of the averaged (a) velocity and (b) acceleration of the column in pipe draining by rigid-column model and elastic-column model

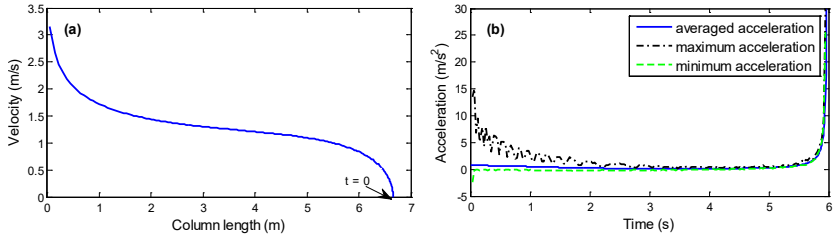

Figure 4 – (a) Outlet velocity vs. column length and (b) histories of acceleration

3.1.2 Head transition

To better understand the dynamics of the flow during emptying, the contribution of the acceleration head $h_a = La/g$ (a is the averaged acceleration among all fluid particles) and the friction head loss $h_f = fLu^2/(2Dg)$ are shown in Fig. 5 together with the driving pressure head and gravity head. Since the downstream valve resistance is zero, the driving head is equal to upstream constant pressure head $h_u = p_{inter}/(\rho g)$. The head transition and the equilibrium of the water column are verified.

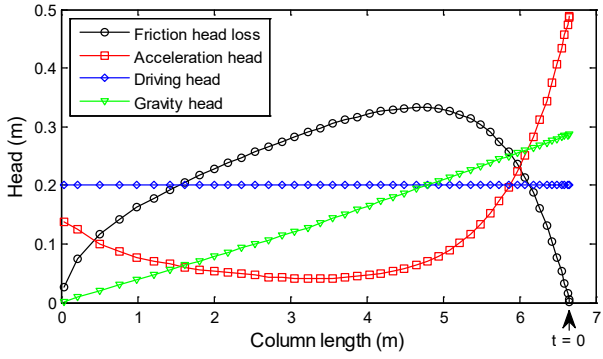

Figure 5 – Contribution of the active heads during the emptying process

3.1.3 Controlled pipe emptying

For controlled pipe emptying through partially opening the downstream valve, the head loss coefficient K_v significantly affects the pipe emptying process as shown in Fig. 6. The valve resistance largely affects the emptying time and maximum velocity, but its effect on the early stage of emptying is insignificant because of the low flow velocities. There is a point (t = 1.25 s) in Fig. 6, where the velocity histories separate. This is because the flow velocity in the early stage is relatively small, and hence the head loss due to valve resistance is unimportant relative to the inertia force.

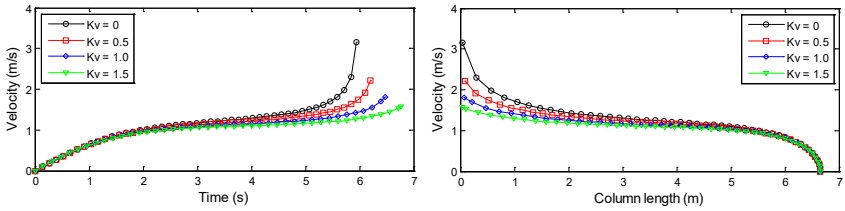

Figure 6 – Effect of valve resistance on column velocity in the emptying process

3.2 Large-scale pipeline

In the second case, the head of the air tank is $H_a = 2$ m of water. The lengths of the two pipes are five times longer than those in the first case. Other parameters are unchanged.
From the simulated velocity history at the valve shown in Fig. 7, the good agreement between the results of the rigid-column model and the elastic-column model is clearly observed. The slight disagreement in the early stage (before the column velocity increases to 1.5 m/s) is due to the effect of water compressibility. It becomes negligible in the rest of the emptying process, when the ratio of the change in internal energy to the change in kinematic energy is much less than one (24).

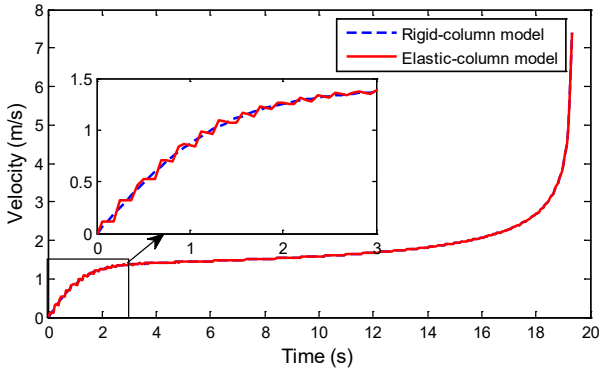

Figure 7 – History of velocity at valve in pipe draining by the elastic-column model

The effect of air tank pressure on the emptying process is shown in Fig. 8. With increasing driving air pressure, the draining process ends earlier with higher velocities and the compressibility effects become negligible earlier. Due to the increased driving pressure, higher velocity changes during one traveling period of the water hammer wave are also seen. These are consistent with expectations.

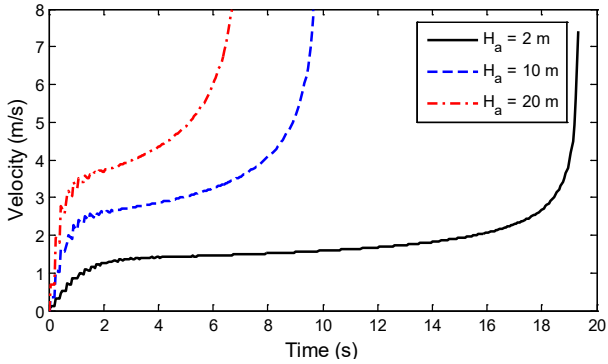

Figure 8 – History of velocities at valve under different driving air pressure

4 SUMMARY AND CONCLUSIONS

Based on the full elastic model, a numerical model in Lagrangian framework is developed for simulating rapid emptying of pipelines with undulating elevation profiles. Since the water column has a shortening length with time, it actually is a transient phenomenon in a computational domain with moving boundary, which is hardly solved using traditional mesh-based methods. Thus, smoothed particle hydrodynamics (SPH) has been applied, which is a meshless second-order accurate method. The image particle method was used to simultaneously ensure complete kernel support and impose boundary conditions. The velocity-Verlet method was employed for time marching to enhance integration accuracy. For validation, two cases of rapid emptying processes of pipelines with large differences in length and driving air head were simulated and the solutions were compared with those of the rigid-column model.

The results show that there is excellent agreement in averaged velocities and accelerations between the rigid-column model and the elastic-column model, confirming the SPH approach. The water column moves as a rigid column during the emptying process of pipelines with small lengths, where the effect of water elasticity is negligible. However, in the emptying process of long pipelines, to capture the water hammer wave during the early emptying stage, the elasticity effect must be taken into account and thus a full elastic model should be employed. Furthermore, if the emptying process is disturbed at a certain point, say by rapid tank or valve operation, the rigid-column theory will fail and an elastic-column model has to be used.

ACKNOWLEDGEMENTS

This work was supported by the Basic Research Program of Qinghai Province under grant no. 2022-ZJ-704. The support is greatly appreciated.

REFERENCES

(1) Wylie, E., Streeter, V. (1993). Fluid transients in systems. New Jersey, NJ: Ed. Prentice Hall.
(2) Fuertes-Miquel, V.S., Coronado-Hernandez, O.E., Mora-Melia, D., Iglesias-Rey, P.L. (2019). Hydraulic modeling during filling and emptying processes in pressurized pipelines: A literature review. Urban Water J., 6(2), 1–13.
(3) Liou, C.P., Hunt, W.A. (1996). Filling of pipelines with undulating elevation profiles. J. Hydraul. Eng., 122(10), 534–539.

(4) Izquierdo, J., Fuertes-Miquel, V.S., Cabrera, E., Iglesias, P.L., Garcia-Serra, J. (1999). Pipeline start-up with entrapped air. J. Hydraul. Res., 37(5), 579–590.
(5) Razak, T., Karney, B.W. (2008). Filling of branched pipelines with undulating elevation profiles. Proc. BHR 10th Int. Conf. Pressure Surges, Edinburgh, 473–487.
(6) Cabrera, E., Abreu, J., Perez, R., Vela, A. (1992). Influence of liquid length variation in hydraulic transients. J. Hydraul. Eng., 118(12), 1639–1650.
(7) Malekpour, A., Karney, B.W. (2008). Rapidly filling analysis of pipelines using an elastic model. Proc. BHR 10th Int. Conf. Pressure Surges, Edinburgh, 539–552.
(8) Malekpour, A., Karney B.W. (2011). Rapid filling analysis of pipelines with undulating profiles by the method of characteristics. Appl. Math., 930460.
(9) Liu, D., Zhou, L., Karney, B.W., Zhang, Q., Ou, C. (2011). Rigid-plug elastic water model for transient pipe flow with entrapped air pocket. J. Hydraul. Res., 49(6), 799–803.
(10) Hou, Q., Zhang L., Tijsseling, A.S., Kruisbrink, A.C.H. (2012). Rapid filling of pipelines with the SPH particle method. Proc. Eng., 31, 38–43.
(11) Hou, Q., Wang, S., Kruisbrink, A.C.H., Tijsseling, A.S (2015). Lagrangian modeling of fluid transients in a pipe with entrapped air. Proc. BHR 12th Int. Conf. Pressure Surges, Dublin, 215–227.
(12) Tijsseling, A.S., Hou, Q., Bozkuş, Z., Laanearu, J. (2016). Improved one-dimensional models for rapid emptying and filling of pipelines. J. Press. Vess. Tech., 138 (3): 1–11.
(13) Laanearu, J., Hou, Q, Tijsseling, A.S. (2015). Experimental and analytical modelling study of air-water front dynamics of two-phase unsteady flows in a large-scale pressurized pipeline. Proc. BHR 12th Int. Conf. Pressure Surges, Dublin, 625–637.
(14) Hou, Q., Tijsseling, A.S., Laanearu, J., Annus, I., Koppel, T., Bergant, A., Vuckovic, S., Anderson, A., van't Westende, J. (2014). Experimental investigation on rapid filling of a large-scale pipeline. J. Hydraul. Eng., 140(11), 04014053.
(15) Laanearu, J., Bergant, A., Annus, I., Koppel, T., van't Westende, J. (2009). Some aspects of fluid elasticity related to filling and emptying of large-scale pipeline. IAHR 3rd Int. Meeting on Cav. & Dyna. Prob. in Hydraul. Mach. & Sys., Brno, 465–474.
(16) Laanearu, J., Annus, I., Koppel, T., Bergant, A., Vuckovic, S., Hou, Q., Tijsseling, A.S., Anderson, A., van't Westende, J. (2012). Emptying of large-scale pipeline by pressurized air. J. Hydraul. Eng., 138(12): 1090–1100.
(17) Tijsseling, A.S., Hou, Q., Bozkus, Z. (2019). Rapid liquid filling of a pipe with venting entrapped gas: analytical and numerical solutions. J. Press. Vess. Tech., 141(4), 041301.
(18) Coronado-Hernandez, O.E., Fuertes-Miquel, V.S., Besharat, M., Ramos, H.M. (2018a). A parametric sensitivity analysis of numerically modelled piston-type filling and emptying of an inclined pipeline with an air valve. Proc. BHR 13th Int. Conf. Pressure Surges, Bordeaux, 949–690.
(19) Fuertes-Miquel, V. S., Coronado-Hernández, O.E., Iglesias-Rey, P.L., Mora-Melia, D. (2019). Transient phenomena during the emptying process of a single pipe with water-air interaction. J. Hydraul. Res., 57(3), 318–326.
(20) Coronado-Hernandez, O.E., Fuertes-Miquel, V.S., Iglesis-Rey, P.L., Martinez-Solano, F.J. (2018b). Rigid water column model for simulating the emptying process in a pipeline using pressurized air. J. Hydraul. Eng.,144(4), 06018004.
(21) Hou, Q., Li, S., Tijsseling, A.S., Laanearu, J. (2020). Discussion of rigid water column model for simulating the emptying process in a pipeline using pressurized air. J. Hydraul. Eng., 146(3), 07020001.
(22) Coronado-Hernandez, O.E., Fuertes-Miquel, V.S., Besharat, M., Ramos, H.M. (2018c). Subatmospheric pressure in a water draining pipeline with an air pocket. Urban Water J., 15(4), 346–352.
(23) Morris, J.P., Patrick, J.F., Zhu, Y. (1997). Modeling low Reynolds number incompressible flows using SPH. J. Comput. Phys, 136(1): 214–226.
(24) Karney, B.W. (1990). Energy relation in transient closed-conduit flow. J. Hydraul. Eng., 116(10), 1180–1196.